SOLAR WALLS WITH VENTILATED TRANSPARENT INSULATION

PERFORMANCE, PROPERTIES, PROBLEMS AND PROSPECTS

Werner J. Platzer, Wilhelm Goerdt
Fraunhofer Institute for Solar Energy Systems,Oltmannsstr. 5, D-79100 Freiburg
Tel. ++49-761-4588-131, Fax ++49-761-4588-132, Werner.Platzer@ise.fhg.de

Abstract – The paper reports experimental and theoretical investigations of a ventilated transparent insulation system using two prototypes of a commercial manufacturer. From the outdoor experiments at the Freiburg facade test unit it can be concluded that the simple stationary theory can be very well used to characterize the system. However, infiltration and thermal bridge effects have to be taken into account. They influence thermal losses and solar gains to some extent and cannot be neglected. Inlet and outlet design is therefore important for building physics as for well as for costs. From computational fluid dynamics information on the outlet dimensions and shape can be deduced. As ventilated transparent insulation is an attractive concept from the point of architecture, as the appearance of the house is not affected by shading devices, the prospects of the system mainly depend on a cost effective and thermally sound solution for the inlet and outlet seals.

1 INTRODUCTION

The application of transparent insulation to massive building walls transforms heat loosers to solar wall heating elements. Due to the angular dependence of the total solar energy transmittance the solar gains in summer are much reduced for vertical South facing walls. However, for large area application they are important and thermal comfort requires usually shading elements. The concept of ventilated transparent insulation was already presented as a possibility to switch from a heating mode in winter to a cooling mode in summer (Liersch, 1993). Within a research and development project commercially made prototypes have been compared.

The optimization of ventilated transparent insulation is depend on several parameters.

- Ventilation gap thickness
- inlet and outlet flow resistance
- thermal bridges
- heat transfer coefficients in the ventilation gap

In order to investigate variations in these effects, simulations and modeling is useful. However, the results need an experimental validation. Therefore temperature and heat flow measurements have been performed time and space resolved at the outdoor facade testing site FASTEST at Fraunhofer. Several prototypes have been used to investigate directly the effects of open and closed inlets and outlets as well as air gap width on the solar efficiency. Computational fluid dynamics simulations were performed to optimize the flow resistance. Comparisons between experimental data and simulations were used to validate the simulation results.

2 FACADE TEST UNIT

Thermal and solar gain investigations under real sky, wind and temperature conditions give insight in the performance of real-size transparent insulation elements. The outdoor facade test site FASTEST has been constructed with eight independent test cabins suitable for such investigations, being situated next to the well-known previous Solar Autonomous House Freiburg.

Fig. 1. View of the FASTEST site in Freiburg, showing four facade elements

Meanwhile several test are being performed. Temperature, energy, radiation, wind and partially daylight data are recorded continously. The evaluation mainly is done using simulations models of the test cabins and parameter identification techniques for the investigated facade elements. In the case of transparent insulation solar walls direct measurement of the heat fluxes into the cabins are performed with heat flux meters.

3 DESCRIPTION OF THE TESTED MODULES

Within the project two different transparent insulation modules including different absorbers were investigated for the use in a ventilated transparent insulation system. One of the prototypes (type A, see Table 1) is very close to a commercial product used without ventilation possibility. The other one (type B) uses an alloy steel thin plate coated with a black chrome selective layer. Because of the selective coating there is a need for an air gap between transparent insulation and absorber in order to decouple heat radiation and convection transport (Platzer, 1992). On the other hand less transparent insulation material is needed in order to reach a similar thermal resistance of the module as type A. A cross-section of the two modules side by side is shown in Figure 1.

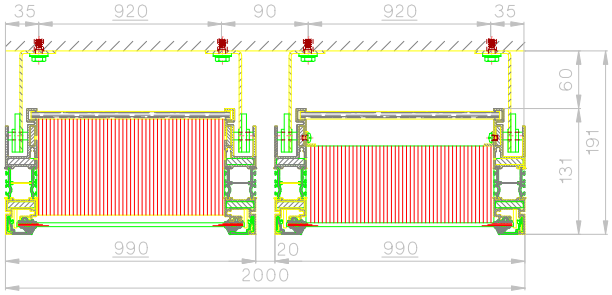

Figure 1: Cross-section of investigated TI-modules left: type A, right: type B (not to scale)

	layers	
parameter	type A	type B
transparent cover	4mm low iron glass 3mm air gap 100mm capillary plate (PC)	4mm low iron glass 80mm capillary plate (PC) 23mm air gap
absorber	Fibre cement plate Eterplan plus grey α_0= 0.72 (± 0.05) ε_0 = 0.90 (± 0.05) ε_b = 0.90 (± 0.05)	Selectively coated steel plate NiCr α_0= 0.95 (± 0.01) ε_0 = 0.10 (± 0.02) ε_b = 0.42 (± 0.05)

Table 1: Specification of the prototypes most important parameters

From the specification values and theoretical calculation we estimated the thermal resistance (without edge effects) at 20°C mean temperature as for type A and for type B. Using measured optical data for the transparent insulation material for different thickness we estimated also the total solar energy transmittance g_B of the modules (in other words: the optical efficiency of the collectors) for normal and hemispherical incidence. Due to the grey colour of the fibre cement absorber the values of g_B are lower for type A.

quantity	type A	type B
R_B (20°C)	1.05 m^2K/W	1.16 m^2K/W
$g_{n,B}$	0.59	0.75
$g_{h,B}$	0.51	0.61

Table 2: Theoretically calculated performance parameter of the modules / collectors

The angular variation of the totalsolar energy transmittance for the two modules is given in Figure 2.

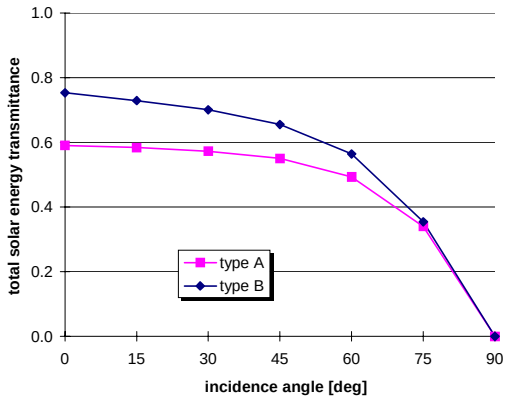

Figure 2: Angular variation of total solar energy transmittance g_B for both modules (theoretical)

4 THEORETICAL MODEL FOR VENTILATED TI

For ventilated transparent insulation there are two modes of operation: In winter time the air space between absorber and wall is closed and the system works as solar wall heating. In summer time inlet (bottom) and outlet (top) of the module are opened and the system is ventilated. The air heats up in contact to the absorber, rises in the air channel and is ventilated away.

Both modes can be treated in a similar way as the traditional solar wall with transparent insulation with the thermal resistance diagram Figure 3. This treatment is used for steady state calculations which are useful for time periods much longer than the time constants of the building elements. In both cases the massive wall is the energy balance position. However, one has to be aware that the effective resistances and g-values of the system do differ from the simple module characteristics of Table 2. The thermal resistance of the air gap between absorber and wall reduces solar gains an increases thermal transistances in the closed winter mode.

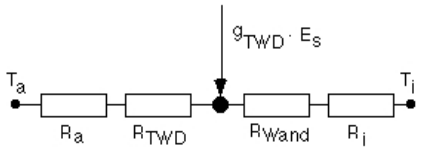

Figure 3: Thermal resistance diagram for transparent insulation

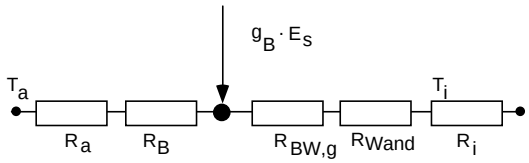

Figure 4: Thermal resistance diagram vor ventilated TI (closed air gap)

Starting from the diagram Figure 4 one can express R_{TWD} and g_{TWD} as follows:

$$R_{c,TWD} = R_B + R_{BW,c}$$

$$g_{c,TWD} = \frac{g_B}{1 + \frac{R_{BW,c}}{R_a + R_B}}$$

For an open, ventilated air channel the situation is more complex as the ventilated air provides a thermal loss possibility for absorber back and massive wall surface (Figure 5):

$$R_{o,TWD} = \frac{R_{W\infty} \cdot \left[(R_a + R_B) \cdot (R_{B\infty} + R_{BW,o}) + R_{B\infty} \cdot R_{BW,o} \right]}{R_{W\infty} + (R_a + R_B) \cdot (R_{B\infty} + R_{BW,o}) + R_{B\infty} \cdot R_{BW,o}}$$

$$g_{o,TWD} = \frac{(R_a + R_B) \cdot R_{B\infty}}{(R_a + R_B) \cdot (R_{B\infty} + R_{BW,o}) + R_{B\infty} \cdot R_{BW,o}} \cdot g_B$$

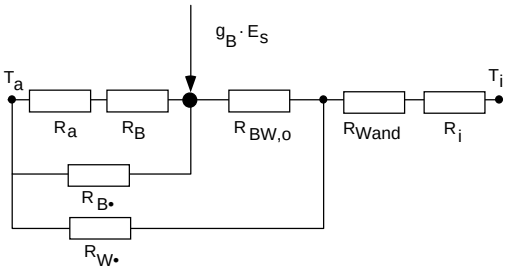

Figure 5: Thermal resistance diagram for ventilated open air channel

5 EXPERIMENTAL RESULTS

In order to investigate the usefulness of the simple stationary theory presented above, we monitored the performance of the two modules in the different modes over a period of several months.

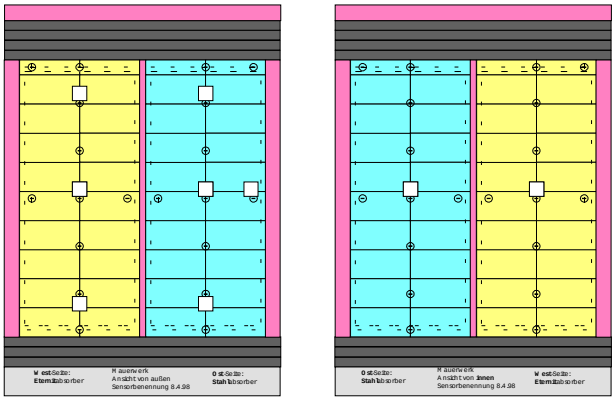

Figure 6: Sketch of modules with sensor locations in the plane of the exterior surface of the wall (square: Heat flux meter; crossed circle: temperature sensor)

The air channel had a width of 60mm. Figure 7 and Figure 8 show typical temperature curves for a day for closed and open mode.

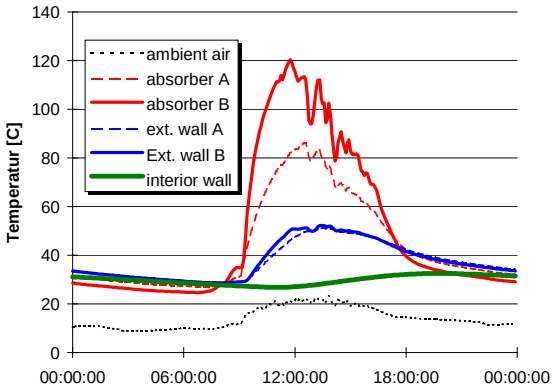

Figure 7: Temperature curves for a sunny October day with in- and outlets closed (both modules; central sensors)

The module type B due to lower rear emissivity of the absorber plate has a reduced capacity to transfer heat to the wall - therfore the absorber temperature is much higher than for module A. The wall surfaces behind the modules reach about the same maximum above 50°C with a small time lag compared to the absorber maximum. The 240mm thick limestone wall stores the heat and releases it to the interior with a time lag of 7 hours at about 20.00h.

Similar is the situation for open air channel. In this case however, it can be observed that the steel absorber keep the wall surface behind cooler than the fibre cement plate: Having a low radiative heat transfer coefficient, the convection air mainly leaving to the ambient, there is not much heat transfer to the wall. The low rear emissivity of the module is positive for the summer situation.

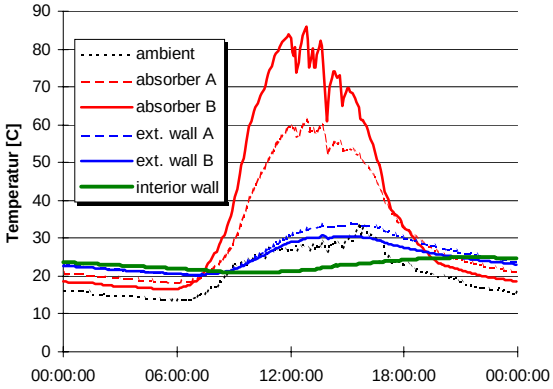

Figure 8: Temperature curves for an August day with ventilated modules (both types; central sensors)

6 EVALUATION

For a quantitative evaluation we use the theory presented earlier using daily averages of measured temperatures and energy flows. We are interested mainly in the overall solar gains of the system module plus wall. The thermal losses are superposed to the gains and result in the measured heat flux q_W at the wall surface:

$$q_W = g_{eff} \cdot \frac{U_{ges}}{U_{TWD}} \cdot E - U_{ges} \cdot (T_R - T_a) = \eta \cdot E - U_{ges} \cdot \Delta T$$

$$U_{ges} = \frac{1}{R_i + R_{Wand} + R_{TWD} + R_a}$$

$$U_{TWD} = \frac{1}{R_{TWD} + R_a}$$

To isolate the solar gains as a function of irradiance on the modules E we rearrange for statistical evaluation:

$$\begin{aligned} q_{sol} &= q_W + U_{ges} \cdot (T_R - T_a) \\ &= q_W + U_{eff} \cdot (T_W - T_a) \\ &= \eta \cdot E \end{aligned}$$

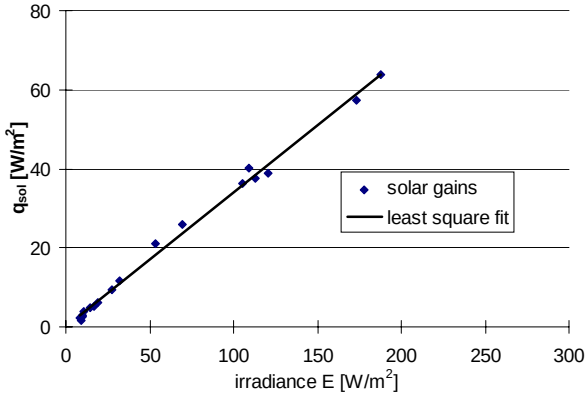

Figure 9: Solar gains of module type A / fibre cement absorber grey

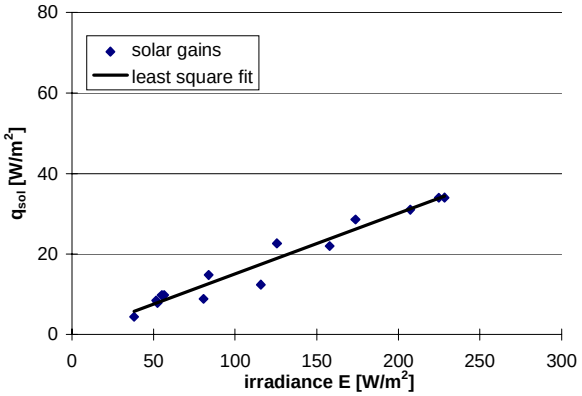

Figure 10: Solar gains of ventilated module type B / selective steel absorber

Figure 9 and Figure 10 show typical diagrams of measured daily averages with a fitted straight line. The quality of the fit indicates that within a period of a few weeks the efficiency can be very well taken as a constant given by the slope of the fit.

The efficiency is reduced to about 40% of the closed state. More important the effective U-value (in theory: U_{TWD}) is largely increased and heat can be removed.

We have tried to identify the thermal resistances (or heat transfer coefficient h = inverse resistances) of Figure 5 for both cases. The results are presented in the following Table 3 and Table 4. This is not a unique solution as we have to fit only two target values for U and η. Nevertheless ist gives an indication of what is not ideal. Even for the closed states the heat transfer coefficients to the ambient air $h_{W,a}$ and $h_{B,a}$ are not zero. This may indicate additional losses due to infiltration of cold ambient air into the air channel. Another interpretation are thermal losses due to thermal bridge effects especially at the outlet. This cannot be separated. The efficiency is appreciably affected. Figure 11 shows the theoretical seasonal variation of the solar efficiency of the solar walls for both module types with these heat transfer coefficients ste to zero. The difference between measured values and the curve indicate (apart from some experimental error) the effect.

type A	**theory**						**experiment**	
mode	$h_{W,a}$	$h_{B,a}$	h_{BW}	U_{eff}	g_{eff}	η	<U>	<η>
open	1.80	4.00	4.40	4.12	0.241	0.181	4.10	0.180
closed	0.10	0.10	6.90	0.98	0.445	0.333	1.00	0.366

Table 3: Thermal parameter type A

type B	**theory**						**experiment**	
mode	$h_{W,a}$	$h_{B,a}$	h_{BW}	U_{eff}	g_{eff}	η	<U>	<η>
open	2.10	4.00	1.60	3.30	0.152	0.117	3.30	0.112
closed	0.10	0.30	4.10	0.98	0.479	0.369	0.95	0.368

Table 4: Thermal parameter type B

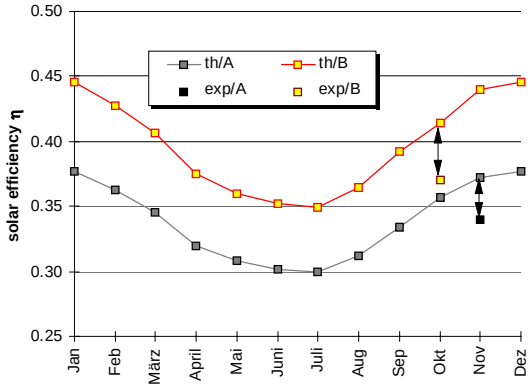

Figure 11: Seasonal variation (Theory) compared with experimental results

7 SIMULATION OF VENTILATION EFFICIENCY

It can be concluded from the previous section that the inlet and outlet construction is very important. Thermal losses due to infiltration and to thermal bridges affect the solar gains. This is one reason why we investigated different options for outlets. Also the summer time ventilation shall be impeded as little as possible. We used computational fluid dynamics (CFD) to investigate our ideas.

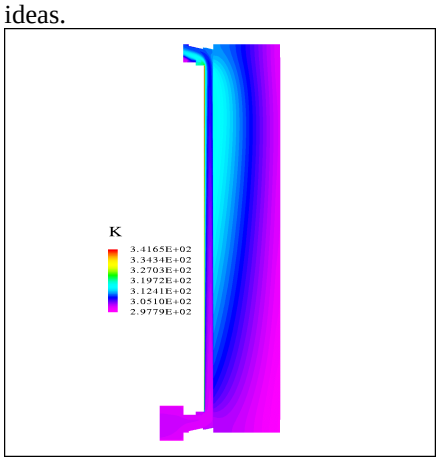

Figure 12: Temperature field of ventilated TI from CFD simulations (dimensions not to scale)

There were three main proposals for outlet seals:

- double flaps with thermal separation (good thermal resistance)
- inflatable rubber tube seal (no mechanical parts)
- rotatable cylinder with thermal break (easy mechanical movement)

The next figure shows a detail of the double flap simulation.

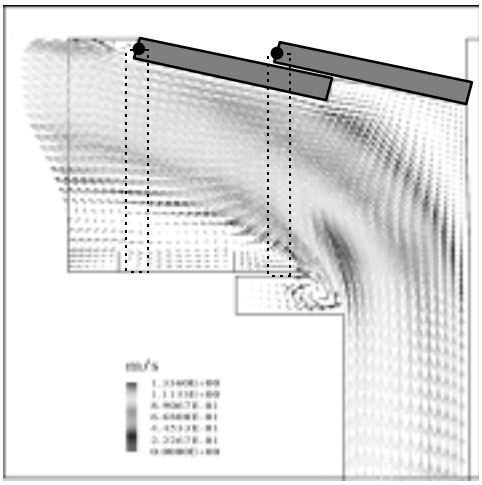

Figure 13: Vector representation of flow field for double flap outlet (double flaps indicated in open position; closed position dashed)

Having the air channel width fixed at 60mm we found that the specific form of the outlet does influence the ventilation (air speed) but not very much (Figure 14). The main parameter seems to be the exit width which should be about the same size as the air channel. An additional rain protection grid reduces air speed appreciably, however.

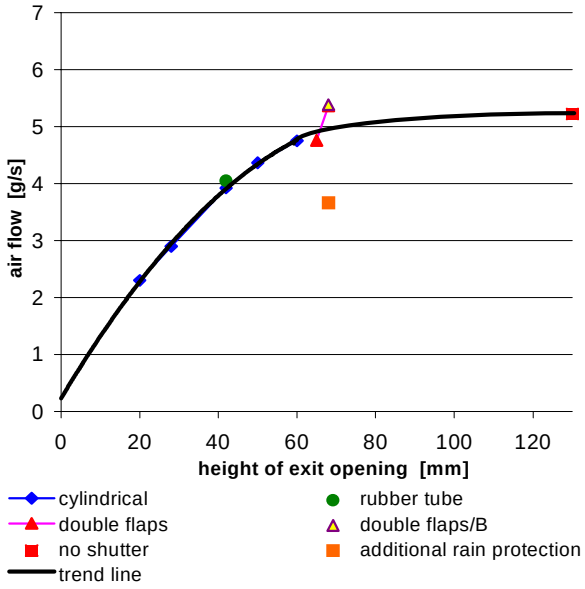

Figure 14: Results for ventilation air flow for different outlet shapes and sizes

8 CONCLUSION

The theoretical models used seem to be sufficiently good to describe the important processes qualitatively and quantitatively. The emissivity of the back side of the absorber has been shown to be important especially for the summer cooling mode. The solar heat gains in summer could be reduced to a very low level with ventilation if the air gap was well designed. The efficiency in the winter mode is critically dependent on air tightness and thermal bridge effects. Quantitative results for the two prototypes are being compared and performance figures for thermal insulation and solar efficiency are presented.

Ventilation of transparent insulation is a viable technical concept for solar wall heating in winter and overheating protection in summer. It is attractive for architectural reasons because does not rely on solar shading products which may affect the appearance of a building facade appreciablly. A critical question for a commercial product is therefore the cost comparison to ordinary transparent insulation with active solar shading. The costs of a thermally insulating and tight-closing outlet are a main parameter. As cost is increased with size the future work will concentrate on minimizing the dimensions without sacrifycing performance, neither in winter nor in summer.

ACKNOWLEDGEMENT

I am grateful to Schweizer Metallbau AG to cooperate with us in this research project. The project was supported by the German Ministry of Research and Technology as well as by the Swiss Bureau für Energiewirtschaft.

REFERENCES

Liersch, G., Dill, F.U.(1993). A ventilated transparent insulation system for wall applications, 6th Int. Conf. On Transparent Insulation TI 6, Birmingham, 3-5 June 1993 (1993) 18-21

Platzer, W.J. (1992). Calculation procedure for collectors with a honeycomb cover of rectangular cross-section, Solar Energy Vol 48 No. 6, pp 381-394